

RSC Advances



This is an *Accepted Manuscript*, which has been through the Royal Society of Chemistry peer review process and has been accepted for publication.

Accepted Manuscripts are published online shortly after acceptance, before technical editing, formatting and proof reading. Using this free service, authors can make their results available to the community, in citable form, before we publish the edited article. This *Accepted Manuscript* will be replaced by the edited, formatted and paginated article as soon as this is available.

You can find more information about *Accepted Manuscripts* in the [Information for Authors](#).

Please note that technical editing may introduce minor changes to the text and/or graphics, which may alter content. The journal's standard [Terms & Conditions](#) and the [Ethical guidelines](#) still apply. In no event shall the Royal Society of Chemistry be held responsible for any errors or omissions in this *Accepted Manuscript* or any consequences arising from the use of any information it contains.



LaF₃-coated Li[Li_{0.2}Mn_{0.56}Ni_{0.16}Co_{0.08}]O₂ as cathode material with improved electrochemical performance for lithium ion batteries

Received 00th January 20xx,
Accepted 00th January 20xx

DOI: 10.1039/x0xx00000x

www.rsc.org/

Qingliang Xie,^a Zhibiao Hu,^b Chenhao Zhao,^b Shuirong Zhang,^a and Kaiyu Liu^{a, b*}

In this article, pristine Li-rich layered oxide Li[Li_{0.2}Mn_{0.56}Ni_{0.16}Co_{0.08}]O₂ porous microspheres had been successfully synthesized by a urea combustion method, and then coated with 1% wt LaF₃ via a facile chemical precipitation route. The structures and morphologies of both pristine and LaF₃ coated Li_{1.2}Mn_{0.54}Ni_{0.16}Co_{0.08}O₂ were performed by X-ray diffractometer (XRD), field-emission scanning electron microscopy (FESEM) and high resolution transmission electron microscope (HR-TEM). The results reveal the obtained particles possess the morphologies of porous microspheres, and a LaF₃ layer with thickness of 5–8 nm is coated on the surface of Li[Li_{0.2}Mn_{0.56}Ni_{0.16}Co_{0.08}]O₂ particle. As lithium ion battery cathodes, the LaF₃ coated sample, compared with the pristine one, has shown a significantly improved electrochemical performances: the initial Columbic efficiency improves from 75.36% to 80.01% and the rate compatibility increased from 57.4 mAh g⁻¹ to an extremely high capacity of 153.5mAh g⁻¹ at 5C. The decreased electrochemical impedance spectroscopy (EIS) reveals that the enhanced electrochemical performance of the surface coating is mainly due to lower charge transfer resistance.

Introduction

In order to meet the requirements of application in electric vehicles (EVs) and hybrid electric vehicles (HEVs), searching for safety, low-cost, long lifetime, high energy density and power density cathode materials has been one of the most important subjects in LIBs^{1–3}. Li-rich layered oxides xLi₂MnO₃·(1-x)LiMO₂ (M = Ni, Co, Mn or combinations) has been regarded as one of the most promising candidate due to its extraordinarily high theoretical discharge capacity of more than 250 mAh g⁻¹ and possess high operating potential over 3.7 V (vs. Li⁺/Li)^{4–6}. However, several drawbacks impede the commercialization of Li-rich cathodes material. The first problem is the enormous irreversible capacity loss of 40–100mAh g⁻¹ in the first cycle depending on the composition when charge up to 4.6 V. The irreversible capacity loss can be attributed to the extraction of Li₂O followed by an elimination of the oxide ion vacancies from the structure during the first charge, leading to fewer insertion-extraction sites of lithium ions in the subsequent discharge process^{7–10}. In addition, the relatively low electron conductivity of Mn-contained layered component and high cut off operating voltage, resulting in

poor rate capability during the electrochemical cycling process^{11,12}.

Previous reports demonstrate that surface coating or modifications is a valid method to enhance the electrochemical performance of cathode materials for LIBs when they cycled on many occasions or charged at a high cut-off voltage (e.g., 4.7 V)^{13–18}. Among all surface modification materials, the metal fluoride such as AlF₃, CaF₂, CeF₃, LiF has been extensively turned out to be an effective approach to improve electrochemical performance of lithium rich layered oxides. Generally, the metal fluoride is believed to suppress the HF corrosion which is responsible for better cycle stability^{19–22}. Furthermore, Zheng et al. reported the AlF₃ coated layer can reduce the activity of extract oxygen and suppressed the electrolyte decomposition at voltages above 4.5V, resulting in improved Coulombic efficiency and cycling stability²³. Sun et al. also indicate that AlF₃ coating layer can induce the transformation of the layer phase to spinel phase. The formation of spinel phase can play a role as fast lithium ion conductor, and help to improve the rate capability²⁴.

LaF₃ is another commonly used metal fluoride. Herein, the opposite ion La³⁺ has an ionic radii of ~106.3 pm, which is larger than Mn⁴⁺, Co³⁺ and Ni²⁺. Thus a slight doping of La³⁺ on the surface of Li-rich layered oxides may lead to the formation of some defects and/or vacancies, and these formed defects and/or vacancies should be helpful for the intercalation/deintercalation of lithium ion²⁵. In the present study, a small amount of LaF₃ (i.e., 1wt%) is coated on the surface of Li[Li_{0.2}Mn_{0.56}Ni_{0.16}Co_{0.08}]O₂ microspheres. Experimental results show that the LaF₃ coated

^a College of Chemistry and Chemical Engineering, Central South University, Changsha, 410083, China

^b College of Chemistry & Materials Science, LongYan University, LongYan 364012, Fujian, China

* E-mail: kaiyuliu67@263.net Tel : 0731-88879616

$\text{Li}_{1.2}\text{Mn}_{0.56}\text{Ni}_{0.16}\text{Co}_{0.08}\text{O}_2$, compared with the pristine $\text{Li}_{1.2}\text{Mn}_{0.56}\text{Ni}_{0.16}\text{Co}_{0.08}\text{O}_2$, exhibit a huge improvement on initial Coulombic efficiency and rate capability. The reasons for the improvements of electrochemical performance via LaF_3 coating were discussed in detail in context.

Experimental

2.1 Preparation of pristine and LaF_3 -coated samples

All raw materials were analytical-grade and used as received. The $\text{Li}[\text{Li}_{0.2}\text{Mn}_{0.56}\text{Ni}_{0.16}\text{Co}_{0.08}]\text{O}_2$ porous sphere were prepared via a facile urea combustion method, described as follows: 0.5112 g LiNO_3 (5% Li excess), 0.2792 g $\text{Ni}(\text{NO}_3)_2 \cdot 6\text{H}_2\text{O}$, 1.301 g aqueous solution of $\text{Mn}(\text{NO}_3)_2$ (50wt%), 0.1397 g $\text{Co}(\text{NO}_3)_2 \cdot 6\text{H}_2\text{O}$ and 1.098 g $\text{CO}(\text{NH}_2)_2$ were dissolved together in 5 ml distilled water to form a uniform solution. Afterwards, the obtained mixed solution was heated in a muffle furnace at 450°C for 40 min under air to remove organic contents. Then, the precursors were ground and further annealed in a muffle furnace at 800°C for 10 h under air, and then cooled down naturally to room temperature.

To prepared LaF_3 -coated $\text{Li}[\text{Li}_{0.2}\text{Mn}_{0.56}\text{Ni}_{0.16}\text{Co}_{0.08}]\text{O}_2$, the as-prepared black powder was immersed into $\text{La}(\text{NO}_3)_3 \cdot n\text{H}_2\text{O}$ aqueous solution under continuous stirring and then drip NH_4F solution into the suspension solution. The pH value of the obtained solution was adjusted to 7.0 by adding ammonia solution. The molar ratio of La to F was regulated to 1:3 and the coating amount of LaF_3 was set to 1 wt% of the parent cathode material. The obtained solution was constantly stirred at 80°C until the solvent was evaporated. Afterwards, the wet powder was dried at 80°C in a vacuum drying oven until the solvent was completely removed. Finally, the dry powders was further annealed in N_2 atmosphere at 450°C for 4 h to gain the LaF_3 -coated $\text{Li}[\text{Li}_{0.2}\text{Mn}_{0.56}\text{Ni}_{0.16}\text{Co}_{0.08}]\text{O}_2$.

2.2 Structure and morphology characterizations

The crystalline phases of the obtained samples were characterized by X-ray diffractometer (DX-2007 LiaoNing DanDong) at a scanning rate of $0.03^\circ/\text{s}$ within 2θ degree of $10\text{--}80^\circ$. SEM images were performed using a Quanta FEG 250 field emission scanning electron microscope (FEI, Electron optics, B.V.). EDX spectrum was performed using an EDAX system. The surface microstructure and selected area electron diffraction (SAED) of coated sample was observed by transmission electron microscope (TEM, JEM-2100F).

2.3 Electrochemical characterization

Electrode slurry was fabricated by mixing 80wt% of active material, 10wt% of carbon black and 10wt% of polyvinylidene difluoride (PVDF) binder with a certain amount of N-methyl-2 pyrrolidone (NMP) solvent. Then the slurry mixture was pasted on an aluminum foil and dried at 80°C for 8 h in a vacuum drying oven. Finally, the dried aluminum foil were cut into round disk with a diameter of 12 mm and the mean mass loading of active materials were about 2.1 mg cm^{-2} . The coin cell (CR2016) was assembled in an argon-filled glove box using pure lithium foils as reference

and counter electrode. Commercial LBC 301 LiPF_6 solution (ShenZhen XinZhouBang) was used as electrolyte and thin polymer acted as separator. The charge-discharge test of assembled cells was performed using NEWARE battery test systems in a range voltage with 2.0–4.7 V at room temperature (about 30°C). Electrochemical impedance spectroscopy (EIS) measurements were performed using an electrochemical workstation (CHI660D, ShangHai ChenHua) in a frequency range of 0.01MHz to 0.1MHz and open circuit voltage of 3.2 V.

Result and discussion

3.1 Structure and morphologies of pristine and LaF_3 -coated $\text{Li}[\text{Li}_{0.2}\text{Mn}_{0.56}\text{Ni}_{0.16}\text{Co}_{0.08}]\text{O}_2$

Fig. 1 shows XRD patterns of pristine and 1wt% LaF_3 -coated $\text{Li}[\text{Li}_{0.2}\text{Mn}_{0.56}\text{Ni}_{0.16}\text{Co}_{0.08}]\text{O}_2$. All the sharp diffraction peaks can be indexed to a hexagonal $\alpha\text{-NaFeO}_2$ type structure with a space group R-3m. Adjacent peaks of (006)/(012) and (108)/(110) were divided clearly,²⁶ indicating that each sample has good crystal structure. Weak XRD peaks observed within 2θ degree of 20 and 25° (marked by *) suggest the periodic occupation of Li^+ ions in the transition metal layers of crystalline LiMO_2 , and the resultant LiMn_6 -typed cation arrangements indicate the coexistence of both crystalline Li_2MnO_3 (also referred to as layered $\text{Li}(\text{Li}_{1/3}\text{Mn}_{2/3})\text{O}_2$) and $\text{LiNi}_{0.4}\text{Co}_{0.2}\text{Mn}_{0.4}\text{O}_2$ ^{21–22}. No LaF_3 and other impurities diffraction peaks can be observed in the XRD pattern, indicating that a little amount of LaF_3 is only coated on the surface of the $\text{Li}[\text{Li}_{0.2}\text{Mn}_{0.56}\text{Ni}_{0.16}\text{Co}_{0.08}]\text{O}_2$, and the bulk structure of the $\text{Li}[\text{Li}_{0.2}\text{Mn}_{0.56}\text{Ni}_{0.16}\text{Co}_{0.08}]\text{O}_2$ remains unchanged after surface modification process.

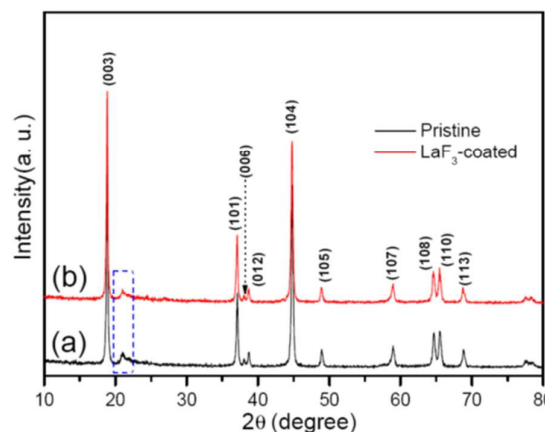


Fig. 1 XRD patterns of (a) pristine and (b) 1wt% LaF_3 -coated $\text{Li}[\text{Li}_{0.2}\text{Mn}_{0.56}\text{Ni}_{0.16}\text{Co}_{0.08}]\text{O}_2$

The morphologies and particle size of the pristine and 1wt% LaF_3 -coated $\text{Li}[\text{Li}_{0.2}\text{Mn}_{0.56}\text{Ni}_{0.16}\text{Co}_{0.08}]\text{O}_2$ were performed by SEM and HR-TEM, as shown in Fig. 2. It can be clearly seen that, the pristine $\text{Li}[\text{Li}_{0.2}\text{Mn}_{0.56}\text{Ni}_{0.16}\text{Co}_{0.08}]\text{O}_2$ are composed of porous microspheres, and these microspheres constructed by numerous nanoparticles have the size of 3–8 μm (Fig. 2a and b). As we known, the porous microsphere structure should be suitable as lithium ion battery

cathode. Firstly, the sphere-like structure can have a good stability during cycling. Secondly, the primary nanoparticles within microspheres can provide a short pathway for the intercalation/deintercalation of lithium ion.²⁷⁻²⁹ Thus, the electrochemical performances should be worth to be expected after surface modification with function materials such as LaF₃.

SEM image of LaF₃-coated porous microspheres was shown in Fig. 2c, compared with the pristine sample (Fig. 2b), a bright coating layer could be observed on the surface of coated, and the gap between nanoparticles is less distinguished due to the existence of the coating layer. To further study the structure of surface coating layer, a high resolution transmission electron microscope (HR-TEM) is carried out, and the result is revealed in Fig. 2d. The lithium rich layered oxides are the nanosized mixture of Li₂MnO₃ and LiMO₂ component. Herein, the Li[Li_{0.2}Mn_{0.56}Ni_{0.16}Co_{0.08}]O₂ also can be denoted as 0.5Li₂MnO₃-0.5LiNi_{0.4}Co_{0.2}Mn_{0.4}O₂. In Fig.2d, the Li₂MnO₃ domain has been successfully captured by HR-TEM, and the lattice fringes with a spacing of 0.43 nm can be assigned to the (020) crystal face of Li₂MnO₃ component. Also, from SAED pattern in Fig.S1, the diffraction dots of (003), (101), (104) and (107) crystal plane can be clearly presented, which are consistent with the XRD pattern in Fig.1. It should be denoted that a little amount of LaF₃ is difficult to be detected by SAED. Especially, the measured thickness of coated layer is about 5-7 nm. In comparison with previous literatures,^{19, 20, 30-32} the thickness of the coating layer was very suitable.

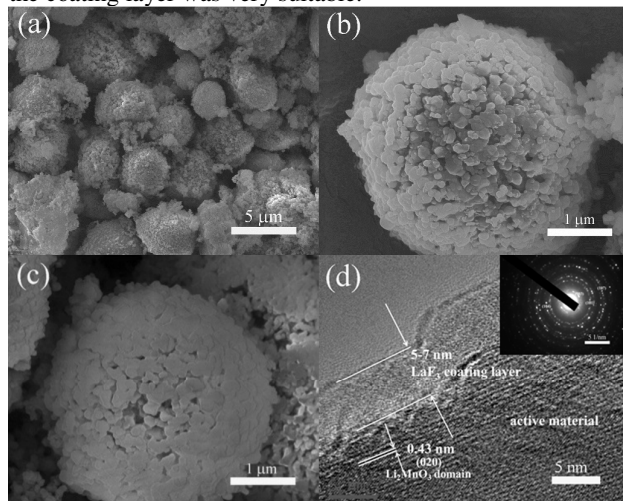


Fig. 2 SEM images of the pristine Li[Li_{0.2}Mn_{0.56}Ni_{0.16}Co_{0.08}]O₂ at a (a) low magnification and (b) high magnification, (c) 1 wt% LaF₃-coated Li[Li_{0.2}Mn_{0.56}Ni_{0.16}Co_{0.08}]O₂, (d) HR-TEM and SAED (selected area electron diffraction) image of LaF₃-coated Li[Li_{0.2}Mn_{0.56}Ni_{0.16}Co_{0.08}]O₂.

In order to further distinguish the difference of the surface structure after coating, The XPS spectrums of pristine and coated samples are carried out as shown in Fig.S2. the characteristic binding energies of La3d and F1s are 834.89 eV and 684.64 eV, respectively, which are in accordance with those of pure LaF₃.³³ Compared with bare

Li[Li_{0.2}Mn_{0.56}Ni_{0.16}Co_{0.08}]O₂, the Ni2p, Co2p and Mn2p peaks (in Fig. S2) of LaF₃-coated Li[Li_{0.2}Mn_{0.56}Ni_{0.16}Co_{0.08}]O₂ have no obvious chemical shift, indicating that the Ni, Co and Mn ion environments in the structure have not been changed. However, the intensity of each peak decreases obviously after coating, which is attributed to the formation of the LaF₃ layer on the surface of Li[Li_{0.2}Mn_{0.56}Ni_{0.16}Co_{0.08}]O₂.¹⁴

Furthermore, the selected area EDS image and corresponding element analysis of 1wt% LaF₃-coated Li[Li_{0.2}Mn_{0.56}Ni_{0.16}Co_{0.08}]O₂ is shown in Fig.3. The calculated element ratio of Ni : Co : Mn in Fig. 4 should be 0.560 : 0.159 : 0.082, which is close to the chemical formula of Li[Li_{0.2}Mn_{0.56}Ni_{0.16}Co_{0.08}]O₂ (i. e., 0.560 : 0.160 : 0.08). The calculated atomic ratio of La : Mn is 1.0 : 50.2 from the EDS analysis, and the theoretical data based on 1wt% LaF₃ coating should be 1.0 : 56.0. These results indicate that the actual element composition of as-prepared pristine and 1wt% LaF₃-coated sample are consistent with the experimental design. It should be emphasized that, the content of O and F is difficult to be accurately detected by EDS. However, the EDS image also shows the coexistence of O and F element.

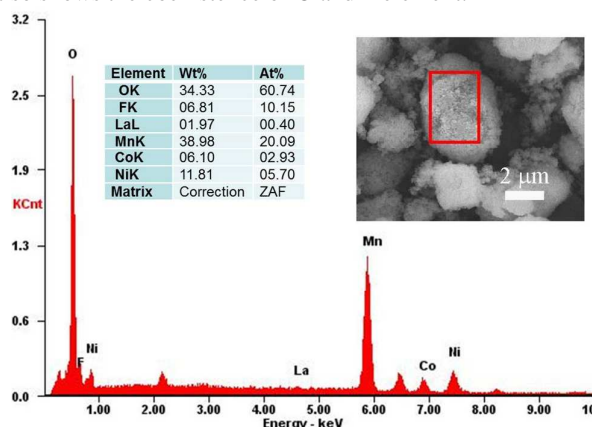


Fig. 3 Element dispersive spectrum (EDS) of 1wt% LaF₃-coated Li[Li_{0.2}Mn_{0.56}Ni_{0.16}Co_{0.08}]O₂, the inserted are the selected area and detailed element analysis.

Fig. 4 comparatively reveals the initial charge-discharge and corresponding dQ/dV curves of pristine and 1%wt LaF₃-coated Li[Li_{0.2}Mn_{0.56}Ni_{0.16}Co_{0.08}]O₂ electrodes within 2.0-4.7 V at 0.1C (1C = 200 mA g⁻¹). The initial charge/discharge capacity of the pristine and 1wt% LaF₃-coated sample are 330/249 and 339/272 mAh g⁻¹ (Fig. 4a), give a Coulombic efficiency of 75.4 and 80.4%, respectively. It is clear that the irreversible capacity loss has been decreased from 81 to 67 mAh g⁻¹. As we know, one of primary disadvantages of LLOs (lithium rich layered oxides) cathodes is the enormous irreversible capacity loss of 40-100 mAh g⁻¹ in the first cycle, and the irreversible capacity loss can be attributed to the extraction of Li₂O followed by an elimination of the oxide ion vacancies from the structure. The surface modification with metal fluoride can reduce the activity of extract oxygen. Thus, the initial Coulombic efficiency of LLOs can be effectively improved. In other words, the improved Coulombic efficiency should be attributed to the fact of that "LaF₃ coated sample, compared with the pristine one, presents higher discharge

capacity under close charge capacity”.

As reported by many literatures^{20, 24, 34}, the surface modification can effectively improve the initial Coulombic efficiency. Zheng et al.²³ reported coating layer can act as a “buffer” layer to enhance the formation of inactive oxygen and restrain the secondary reaction of electrolyte oxidation caused by active oxygen species. Thus, an improved Coulombic efficiency can be expected.

Fig. 4b is the dQ/dV curves of pristine and coated sample. During the first charge process, an anodic peak nearby 4.00 V can be ascribed to the de-intercalation of Li⁺ ions from LiNi_{0.4}Co_{0.2}Mn_{0.4}O₂ phase and the oxidation of Ni²⁺ ions, and the sharp anodic peak within 4.50–4.52 V corresponds to the transformation of Li₂MnO₃ to layered MnO₂ and the oxidation of Co³⁺ ions. In the initial discharge process, two cathodic peaks around 3.75 and 3.30 V indicate the intercalation of Li⁺ ions into layered LiNi_{0.4}Co_{0.4}Mn_{0.4}O₂ and previously formed MnO₂, respectively. Compared with pristine Li[Li_{0.2}Mn_{0.56}Ni_{0.16}Co_{0.08}]O₂, the coated sample has a high discharge voltage (Fig. 4b, red curve), which demonstrates that the coating layer can reduce the polarization to a certain degree.

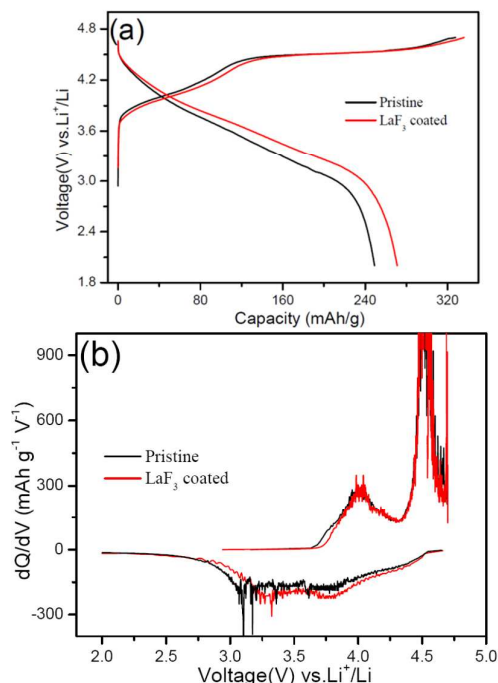


Fig. 4 The initial charge/discharge voltage profiles and corresponding differential capacity (dQ/dV) curves of pristine Li[Li_{0.2}Mn_{0.56}Ni_{0.16}Co_{0.08}]O₂ and 1wt% LaF₃-coated Li[Li_{0.2}Mn_{0.56}Ni_{0.16}Co_{0.08}]O₂ electrodes at a current density of 0.1C between 2.0 and 4.7V.

The discharge capacity and cycling performance of the electrode materials at an elevated current density are significant parameter for cathode. The discharge capacity and cycling stability of pristine and 1wt% LaF₃-coated Li[Li_{0.2}Mn_{0.56}Ni_{0.16}Co_{0.08}]O₂ are studied, as shown in Fig. 5. Similar with the discharge capacity at low current density (Fig. 4a), the LaF₃-coated samples have a higher discharge

capacity (182.1 mAh g⁻¹) and initial Coulombic efficiency of 75.36% compared to the pristine samples (158.0 mAh g⁻¹, 70.01%) at 1C (Fig. 5a). The cycling stability of these samples is shown in Fig. 5b. A residual discharge capacity of 161.7 and 193.0 mAh g⁻¹ can be retained after 50 cycles. In comparison with initial value (158.0 and 182.1 mAh g⁻¹), the cycling stability of both two samples is excellent, especially LaF₃-coated sample.

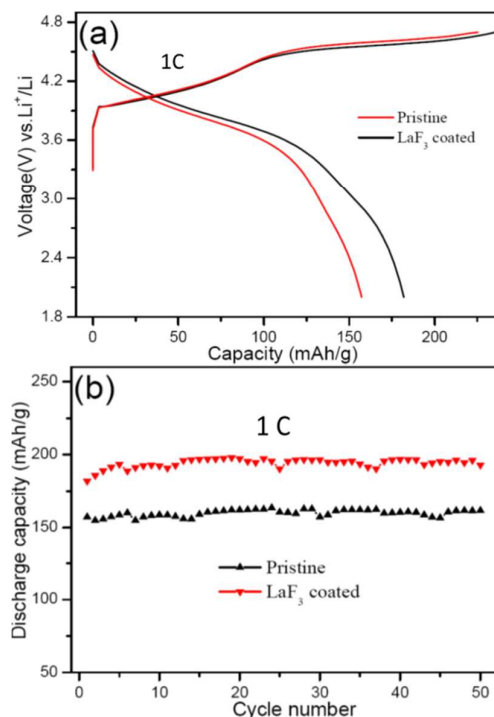


Fig. 5 (a) The initial charge/discharge curves and (b) cycling performances of the Li[Li_{0.2}Mn_{0.56}Ni_{0.16}Co_{0.08}]O₂ and 1wt% LaF₃-coated Li[Li_{0.2}Mn_{0.56}Ni_{0.16}Co_{0.08}]O₂ electrodes within 2.0–4.7 V at 1C.

Although the Li-rich layered xLi₂MnO₃·(1-x)LiMO₂ has an extraordinarily high theoretical discharge capacity of more than 250 mAh g⁻¹ and possess high operating potential of 4.6–4.8 V (vs. Li⁺/Li), the poor rate capacity was one of the most important drawback that impede the commercialization of this cathode materials^{35–37}. In this paper, the rate capability of the pristine and LaF₃-coated Li[Li_{0.2}Mn_{0.56}Ni_{0.16}Co_{0.08}]O₂ were performed in Fig. 6a. Apparently, the discharge capacity decrease of each sample with elevated current density. The LaF₃-coated Li[Li_{0.2}Mn_{0.56}Ni_{0.16}Co_{0.08}]O₂ have much better rate compatibility than the pristine sample. The LaF₃-coated electrode exhibits a stable discharge capacity of 273.2, 229.3, 202.7 or 178.2 mAh g⁻¹ at current density 0.1C, 0.5C, 1C or 2C, respectively. Even when the current density is increased to a high value of 5C, the electrode still delivers a high discharge capacity of 153.5 mAh g⁻¹. While, the pristine sample only shows a discharge capacity 121 or 58.2 mAh g⁻¹ at current density of 2C or 5C. As shown in Fig. 6b and c, the discharge profiles at various C rates of pristine and 1wt% LaF₃-coated Li[Li_{0.2}Mn_{0.56}Ni_{0.16}Co_{0.08}]O₂. The capacity and

voltage decay with elevated current density has been denoted by arrow, and it can be seen that the pristine sample has a more serious decay. According to above results, the rate capability of $\text{Li}[\text{Li}_{0.2}\text{Mn}_{0.56}\text{Ni}_{0.16}\text{Co}_{0.08}]\text{O}_2$ has been greatly improved by surface coating with 1wt%. Maybe, the LaF_3 can act as a fast Li ion conductor and/or induce the formation of spinel Li-Ni-Mn-O oxide³⁸⁻⁴⁰, and which facilitate the insertion/extraction of Li ion within the interface of electrode material and electrolyte.

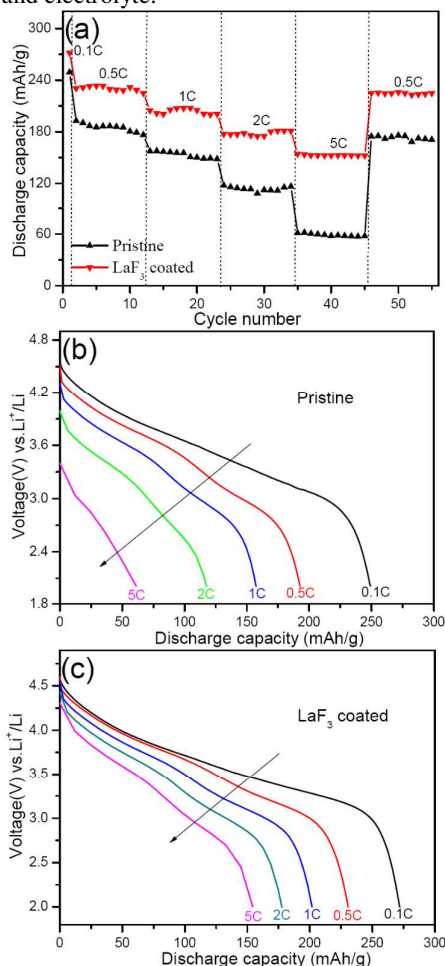


Fig. 6 (a) Rate capability of the pristine $\text{Li}[\text{Li}_{0.2}\text{Mn}_{0.56}\text{Ni}_{0.16}\text{Co}_{0.08}]\text{O}_2$ and 1wt% LaF_3 -coated $\text{Li}[\text{Li}_{0.2}\text{Mn}_{0.56}\text{Ni}_{0.16}\text{Co}_{0.08}]\text{O}_2$ electrodes, the initial discharge profiles of (b) $\text{Li}[\text{Li}_{0.2}\text{Mn}_{0.56}\text{Ni}_{0.16}\text{Co}_{0.08}]\text{O}_2$ and (c) LaF_3 -coated $\text{Li}[\text{Li}_{0.2}\text{Mn}_{0.56}\text{Ni}_{0.16}\text{Co}_{0.08}]\text{O}_2$ at a series of current densities and the arrow (inset) denotes a voltage decrease with increased current densities.

With the purpose of further investigate the mechanism of enhanced electrochemical performance of LaF_3 -coated $\text{Li}[\text{Li}_{0.2}\text{Mn}_{0.56}\text{Ni}_{0.16}\text{Co}_{0.08}]\text{O}_2$, Fig. 7 shows the electrochemical impedance spectroscopy (EIS) of the pristine and LaF_3 -coated $\text{Li}[\text{Li}_{0.2}\text{Mn}_{0.56}\text{Ni}_{0.16}\text{Co}_{0.08}]\text{O}_2$, collected after 3 charge-discharge cycles at 0.1C. It should be mentioned out that the spectroscopy is fitted using impedance matching software ZSimDemo 3.30 original spectrum in Fig.S3. The high-frequency semicircle and low-frequency slope line was given

by the Nyquist plots, in which the high-frequency semicircle is related to the charge transfer resistance (R_{ct}) in the electrode/electrolyte and the low-frequency slope line on behalf of the impedance of the lithium ion diffusion in bulk electrode materials. Obviously, compared to the pristine samples, the LaF_3 -coated samples have a much smaller R_{ct} value. The R_{ct} value of the pristine samples was 116.2 Ω , while the LaF_3 -coated samples exhibit an R_{ct} value of 89.66 Ω . As mentioned above, it demonstrates that the LaF_3 acted as a very stable conductor layer to improve the electrochemical conductivity of as-prepared $\text{Li}[\text{Li}_{0.2}\text{Mn}_{0.56}\text{Ni}_{0.16}\text{Co}_{0.08}]\text{O}_2$ ^{24, 35, 41}. That it is the reason why the LaF_3 coating layer results in the excellent rate compatibilities and higher columbic efficiency of the electrode.

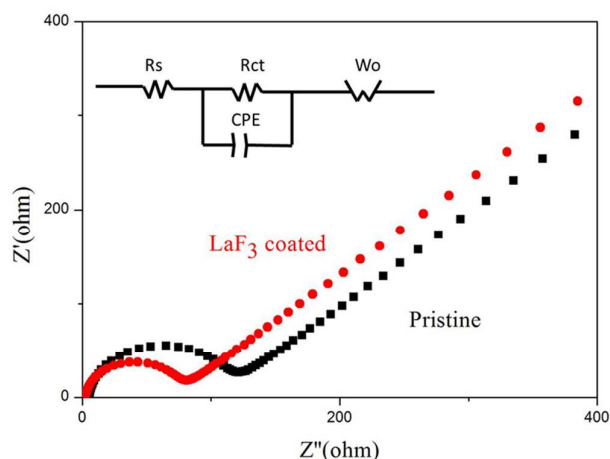


Fig. 7 Electrochemical impedance spectroscopy (EIS) and the used equivalent circuit (inset) of pristine and LaF_3 -coated $\text{Li}[\text{Li}_{0.2}\text{Mn}_{0.56}\text{Ni}_{0.16}\text{Co}_{0.08}]\text{O}_2$ after 3 cycles before charge.

Conclusions

As we all know, the initial columbic efficiency and the poor rate performance are the main drawbacks that impeding the possible commercialization of lithium rich layered oxides such as $\text{Li}[\text{Li}_{0.2}\text{Mn}_{0.56}\text{Ni}_{0.16}\text{Co}_{0.08}]\text{O}_2$. In this paper, the pristine $\text{Li}[\text{Li}_{0.2}\text{Mn}_{0.56}\text{Ni}_{0.16}\text{Co}_{0.08}]\text{O}_2$ porous microspheres has been successfully synthesized by a urea combustion method and then uniformly coated with LaF_3 using a simple chemical precipitation method. The coating layer has a reasonable thickness of 5-7 nm. As lithium ion battery cathode, the LaF_3 -coated $\text{Li}[\text{Li}_{0.2}\text{Mn}_{0.56}\text{Ni}_{0.16}\text{Co}_{0.08}]\text{O}_2$ exhibits greatly enhanced electrochemical performance compared with pristine sample. The initial columbic efficiency has been improved from 75.36% to 80.01%. Especially, the discharge capacity increases from 57.4 to 153.5 mAh g^{-1} at 5C. Maybe, the coating layer of LaF_3 can act as “buffer” and “conductor” to enhance initial Coulombic efficiency and rate capability.

Acknowledgements

This work was financially supported by the Science and Technology Program of LongYan (2014LY36) and the School Research Program of LongYan University (LC2013008).

References

1. A. Ito, D. Li, Y. Ohsawa and Y. Sato, *Journal of Power Sources*, 2008, **183**, 344-346.
2. T. A. Arunkumar, E. Alvarez and A. Manthiram, *J. Mater. Chem.*, 2008, **18**, 190-198.
3. J. Bareno, C. H. Lei, J. G. Wen, S. H. Kang, I. Petrov and D. P. Abraham, *Advanced materials*, 2010, **22**, 1122-1127.
4. N. Yabuuchi, K. Yoshii, S. T. Myung, I. Nakai and S. Komaba, *Journal of the American Chemical Society*, 2011, **133**, 4404-4419.
5. H. Kobayashi, Y. Takenaka, Y. Arachi, H. Nitani, T. Okumura, M. Shikano, H. Kageyama and K. Tatsumi, *Solid State Ionics*, 2012, **225**, 580-584.
6. L. Simonin, J.-F. Colin, V. Ranieri, E. Canévet, J.-F. Martin, C. Bourbon, C. Baetz, P. Strobel, L. Daniel and S. Patoux, *Journal of Materials Chemistry*, 2012, **22**, 11316.
7. S. Rajarathinam, S. Mitra and R. K. Petla, *Electrochimica Acta*, 2013, **108**, 135-144.
8. X. Zhang, C. Yu, X. Huang, J. Zheng, X. Guan, D. Luo and L. Li, *Electrochimica Acta*, 2012, **81**, 233-238.
9. J. Wang, G. Yuan, M. Zhang, B. Qiu, Y. Xia and Z. Liu, *Electrochimica Acta*, 2012, **66**, 61-66.
10. J.-L. Liu, J. Wang and Y.-Y. Xia, *Electrochimica Acta*, 2011, **56**, 7392-7396.
11. D. Mohanty, A. S. Sefat, S. Kalnaus, J. Li, R. A. Meisner, E. A. Payzant, D. P. Abraham, D. L. Wood and C. Daniel, *Journal of Materials Chemistry A*, 2013, **1**, 6249.
12. S. Hy, W.-N. Su, J.-M. Chen and B.-J. Hwang, *The Journal of Physical Chemistry C*, 2012, **116**, 25242-25247.
13. Y. Chen, G. Xu, J. Li, Y. Zhang, Z. Chen and F. Kang, *Electrochimica Acta*, 2013, **87**, 686-692.
14. X.-H. Liu, L.-Q. Kou, T. Shi, K. Liu and L. Chen, *Journal of Power Sources*, 2014, **267**, 874-880.
15. J. Liu, Q. Wang, B. Reeja-Jayan and A. Manthiram, *Electrochemistry Communications*, 2010, **12**, 750-753.
16. Y. J. Kang, J. H. Kim, S. W. Lee and Y. K. Sun, *Electrochimica Acta*, 2005, **50**, 4784-4791.
17. W. C. West, J. Soler, M. C. Smart, B. V. Ratnakumar, S. Firdosy, V. Ravi, M. S. Anderson, J. Hrbacek, E. S. Lee and A. Manthiram, *Journal of The Electrochemical Society*, 2011, **158**, A883.
18. Q. Y. Wang, J. Liu, A. V. Murugan and A. Manthiram, *Journal of Materials Chemistry*, 2009, **19**, 4965.
19. X. Liu, J. Liu, T. Huang and A. Yu, *Electrochimica Acta*, 2013, **109**, 52-58.
20. C. Lu, H. Wu, Y. Zhang, H. Liu, B. Chen, N. Wu and S. Wang, *Journal of Power Sources*, 2014, **267**, 682-691.
21. P. Mohan and G. Paruthimal Kalaignan, *Ceramics International*, 2014, **40**, 1415-1421.
22. T. Shi, Y. Dong, C.-M. Wang, F. Tao and L. Chen, *Journal of Power Sources*, 2015, **273**, 959-965.
23. Z. Lu and J. R. Dahn, *Journal of The Electrochemical Society*, 2002, **149**, A815-A822.
24. Y. K. Sun, M. J. Lee, C. S. Yoon, J. Hassoun, K. Amine and B. Scrosati, *Advanced materials*, 2012, **24**, 1192-1196.
25. T. Ohnishi, K. Mitsuishi, K. Nishio and K. Takada, *Chemistry of Materials*, 2015, **27**, 1233-1241.
26. O. Toprakci, H. A. K. Toprakci, Y. Li, L. Ji, L. Xue, H. Lee, S. Zhang and X. Zhang, *Journal of Power Sources*, 2013, **241**, 522-528.
27. W.-M. Chen, L. Qie, Y. Shen, Y.-M. Sun, L.-X. Yuan, X.-L. Hu, W.-X. Zhang and Y.-H. Huang, *Nano Energy*, 2013, **2**, 412-418.
28. J. Liu, L. Chen, M. Hou, F. Wang, R. Che and Y. Xia, *Journal of Materials Chemistry*, 2012, **22**, 25380.
29. X. Wei, S. Zhang, Z. Du, P. Yang, J. Wang and Y. Ren, *Electrochimica Acta*, 2013, **107**, 549-554.
30. S. Zhao, Y. Bai, L. Ding, B. Wang and W. Zhang, *Solid State Ionics*, 2013, **247-248**, 22-29.
31. S.-H. Kang and M. M. Thackeray, *Electrochemistry Communications*, 2009, **11**, 748-751.
32. S. Francis Amalraj, B. Markovsky, D. Sharon, M. Talianker, E. Zinigrad, R. Persky, O. Haik, J. Grinblat, J. Lampert, M. Schulz-Dobrick, A. Garsuch, L. Burlaka and D. Aurbach, *Electrochimica Acta*, 2012, **78**, 32-39.
33. H. Yu, Y. Shen, Y. Cui, H. Qi, J. Shao and Z. Fan, *Applied Surface Science*, 2008, **254**, 1783-1788.
34. B. Xiao, J. Liu, Q. Sun, B. Wang, M. N. Banis, D. Zhao, Z. Wang, R. Li, X. Cui, T.-K. Sham and X. Sun, *Advanced Science*, 2015, n/a-n/a.
35. J. W. Min, J. Gim, J. Song, W.-H. Ryu, J.-W. Lee, Y.-I. Kim, J. Kim and W. B. Im, *Electrochimica Acta*, 2013, **100**, 10-17.
36. S. K. Martha, J. Nanda, Y. Kim, R. R. Unocic, S. Pannala and N. J. Dudney, *Journal of Materials Chemistry A*, 2013, **1**, 5587.
37. B. Liu, Q. Zhang, S. He, Y. Sato, J. Zheng and D. Li, *Electrochimica Acta*, 2011, **56**, 6748-6751.
38. K. Kubota, T. Kaneko, M. Hirayama, M. Yonemura, Y. Imanari, K. Nakane and R. Kanno, *Journal of Power Sources*, 2012, **216**, 249-255.
39. B. Song, Z. Liu, M. O. Lai and L. Lu, *Physical chemistry chemical physics : PCCP*, 2012, **14**, 12875-12883.
40. D. Mohanty, S. Kalnaus, R. A. Meisner, K. J. Rhodes, J. Li, E. A. Payzant, D. L. Wood and C. Daniel, *Journal of Power Sources*, 2013, **229**, 239-248.

Journal Name

Paper

41. Q. Q. Qiao, H. Z. Zhang, G. R. Li, S. H. Ye, C. W. Wang and X. P. Gao, *Journal of Materials Chemistry A*, 2013, **1**, 5262.

RSC Advances Accepted Manuscript